X-662-74-231

PREPRINT

NASA TM X- 70731

HEAVY SOLAR COSMIC RAYS IN THE JANUARY 25, 1971 SOLAR FLARES

CHARLES J. PELLERIN, JR.

(NASA-TM-X-70731) HEAVY SOLAR COSMIC RAYS IN THE JANUARY 25, 1971 SOLAR FLARES (NASA) 32 p HC $4.75 CSCL 03B

N74-32244

Unclas

G3/29 46689

AUGUST 1974

GODDARD SPACE FLIGHT CENTER
GREENBELT, MARYLAND

Heavy Solar Cosmic Rays in the January 25, 1971 Solar Flare

Charles J. Pellerin, Jr.

NASA/Goddard Space Flight Center
Greenbelt, MD 20771

ABSTRACT

A detailed study of the charge composition of heavy solar cosmic rays measured in the January 25, 1971 solar flare including differential fluxes for the even charged nuclei from carbon through argon is presented. The measurements are obtained for varying energy intervals for each nuclear species in the energy range from 10 to 35 MeV/nucleon. In addition, abundances relative to oxygen are computed for all the above nuclei in the single energy interval from 15 to 25 MeV/nucleon. This interval contains measurements for all of the species and as a result requires no spectral extrapolations. An upper limit for the abundance of calcium nuclei is also presented.

These measurements, when combined with other experimental results, enable the energy dependence of abundance measurements as a function of nuclear charge to be discussed. It is seen that at energies above about 10 MeV/nucleon, the variations of abundance ratios are limited to about a factor of 3 from flare to flare, in spite of large variations in other characteristics of these solar events.

1. Introduction

The existence of multicharged nuclei in solar cosmic rays was first established as part of the early SPICE (Solar Particle Intensity and Composition Experiment) experiment. This experiment involved the launching of sounding rockets into large solar particle events to expose nuclear emulsion stacks to the incident particle radiation. Measurements of the relative abundances of these heavy, multicharged particles were made at energies above 40 MeV/nucleon several times in major solar flares occuring in 1960 and 1969 (see, for example Fichtel and Guss, 1961; Biswas et al., 1962, 1963; Bertsch et al. 1972). An outstanding result of these measurements at energies $\geq$ 40 MeV/nucleon was the observation that the relative abundances of multicharged nuclei were constant within the experimental uncertainties from flare to flare in spite of large variations in such parameters as the flare size and proton to helium ratio. Furthermore, these abundance ratios were the same within experimental uncertainties as those measured in the solar atmosphere using spectroscopic methods.

This constancy may result from the fact that rules of nuclear stability provide for the even-charged nuclei to be generally much more abundant than the odd-charged nuclei in the sun and, consequently, the most abundant isotopes of multicharged nuclei observed in solar cosmic rays have charge-to-mass ratios that are almost constant provided the nuclei are fully stripped (the exception is iron which has a somewhat smaller charge-to-mass ratio). Since all particles with the same charge-to-mass ratio will have an identical rigidity at the same velocity, each species will be treated identically by electromagnetic forces irrespective of the complexity of the magnetic field. An exception to this would be the energy losses that a particle undergoes from Coulomb interactions, but this effect does not appear to be important, particularly for the propagation. It should be noted that all of the nuclei will be essentially fully stripped at energies above about 15 MeV/nucleon if they pass through even about a milligram/cm^2 of matter (Heckman et al., 1963).

More recently, detailed solar particle abundances of multicharged nuclei have been measured with satellite borne detectors (Teegarden et al., 1973; Mogro-Campero and Simpson, 1972) at somewhat lower energies of about 20 MeV/nucleon. These measurements differed from the sounding rocket measurements in that the small geometric factors of the satellite instrumentation generally required that abundances be computed with data summed over the duration of a flare in order to reduce the statistical uncertainties, in contrast to the sounding rocket exposures which were exposures of about four minutes near flare particle flux maxima. These satellite results showed areas of disagreement with the previous sounding rocket results as well as variability in the abundance ratios from flare to flare.

In addition there have been recent measurements of solar cosmic rays at still lower energies ($\lesssim$ 10 MeV/nucleon) which show abundance ratio variations which appear to grow larger as the energy of the measurements decreases. These measurements include data from plastic detectors flown on SPICE sounding rockets (Crawford et al., 1972;

Price et al., 1973) as well as satellite measurements (Hovestadt et al., 1973).

The variability of solar cosmic rays has also been studied from the point of view of the ratios of charge groups, where the individual nuclei are unresolved (e.g. Bertsch et al., 1974). These observations include other SPICE exposures as well as satellite experiments (e.g. Bertsch et al., 1973a, 1973b, 1972; Armstrong and Krimigis, 1971; Armstrong et al., 1972; Braddy et al., 1973). While such observations are able to address the question of solar particle abundance variations, they are unable to make detailed comparisons with solar spectroscopic measurements or to treat the question of the detailed Z dependence of the observed variations at low energies.

In order to further study the processes of solar acceleration as a function of particle energy and charge, this experiment undertakes a detailed charge measurement near the maximum particle intensity in the January 25, 1971 solar flare. The even-charged nuclei from carbon through calcium are identified and differential energy spectra are presented for the nuclei where the statistical uncertainties are sufficiently small. The elemental abundances for these nuclei are then calculated in the common energy interval from 15 to 25 MeV/nucleon.

2. Experimental Procedure

Nuclear emulsion stacks exposed to the intense particle radiation of the January 25, 1971 solar flare at 1512 UT were analyzed for this experiment. The stacks were carried above the atmosphere by a NIKE-APACHE sounding rocket launched from Ft. Chruchill, Manitoba. By opening a protective nosecone while the payload was above the atmosphere, a 245 second sample of the incident particle radiation was obtained. The payload was maintained in a nearly vertical direction for the duration of the emulsion exposure by means of a 6 rps spin imposed along the longitudinal axis of the payload.

The top emulsion pellicle in a stack composed of Ilford K.5 emulsion was scanned over an area of about 10 cm^2 to visually select tracks resulting from nuclei with $Z > 2$. The tracks were also required to have entered the stack from the upper hemisphere and to have entrance angles of from 10 to 60 degrees with respect to the emulsion surface. In order to ensure that there was a sufficient length of track for charge analysis, the tracks were also required to have a length of 50 μm projected onto the emulsion surface.

The selected tracks were analyzed with an automated measuring system which measured the track width as a function of residual range. The track width information was obtained by viewing the emulsion image with a television camera. The analog signal from the camera was converted into binary information with electronic descrimination circuitry. These data were then analyzed with a digital computer to extract the track width information. As described in detail in Pellerin (1974), the Z dependence of track width as a function of residual range is seen to be well approximated by a power law. A simple model then allows the charges of the incident nuclei to be calculated. The measurement of the total range of each particle then determines the kintetic energy. This experimental result comprises the analysis of about 1400 particles.

3. Results

The differential fluxes for carbon, oxygen, neon, and magnesium are shown in Figure 1. As is generally the case with dE/dX by E detectors, the energy threshold for which each nuclear species is measured increases with charge. The data from this experiment range from about 10 to 35 MeV/nucleon with all detected nuclear species having flux values in the interval from about 15 to 25 MeV/nucleon. Power law functions were found to yield reasonably good fits to all of the data given the statistical uncertainties. The figure also contains straight lines corresponding to a spectral index of 3.5 to aid in comparing the spectral shapes. There is an apparent tendency of the spectral index for each nuclear species to increase with charge. Least-squares fits with power law spectra for each of the nuclear species in Figure 1 were made in the common energy interval from 15 to 25 MeV/nucleon, and yield the spectral indicies shown in Figure 2. The figure also has a datum for helium for the same flare from Bertsch el al., (1973a). While the tendency of the spectra to steepen with increasing charge is apparent, the data are also consistent with a constant spectral index.

This experimental technique did not result in a good separation of nitrogen nuclei from carbon and oxygen nuclei. The carbon and oxygen fluxes were therefore corrected by assuming that the nitrogen nuclei were distributed into the carbon and oxygen nuclei in proportion to the number of nuclei identified as carbon and oxygen. The nitrogen abundance was assumed to be 19% of oxygen, a value observed in many experiments in this approximate energy interval (e.g. Bertsch et al., 1972, Teegarden et al., 1973).

The differential fluxes of silicon, sulphur, and argon nuclei are shown in Figure 3. No nuclei identifiable as calcium were found. As in the previous figure, a line representing a power law spectrum with an index of 3.5 is shown with the data as a reference.

The iron ($22 \leq Z \leq 28$) data shown in Figure 3 are from Bertsch et al. (1973a). These data are shown because they represent measurements made in the same emulsion plate as the measurements presented here, but have better statistical accuracy since the entire available emulsion area was scanned. The measured fluxes for all the nuclei discussed above are summarized in Table 1.

Crawford et al. (1972) have measured particles during the same flight exposure using different particle detectors, and it is useful to compare their values with the results in this experiment in the overlapping energy intervals. This can be done only for oxygen, silicon and iron. The iron result has been reported earlier by Bertsch et al. (1973a) and a comparison showing good agreement was made in that paper. Figure 4 shows the results of Crawford et al., (1972) and the data obtained in this experiment for oxygen and silicon nuclei. It can be seen that the two experimental techniques yield results that are in good agreement.

In the mutual energy interval for all of the species, 15 to 25 MeV/nucleon, the relative abundances can be calculated without spectral extrapolation. The relative abundance calculation is performed in the following manner. A power-law function is fitted to the oxygen flux

TABLE 1 Particle Fluxes

OXYGEN

DJ/DE*	Error	Energy+
0.0479	0.0055	12.4
0.0394	0.0059	13.2
0.0378	0.0049	14.0
0.0340	0.0042	15.0
0.0244	0.0030	16.1
0.0211	0.0023	17.8
0.0111	0.0014	20.2
0.0043	0.0006	24.5

CARBON

DJ/DE*	Error	Energy+
0.0359	0.0056	11.3
0.0320	0.0045	12.0
0.0160	0.0018	13.3
0.0142	0.0020	15.2
0.0083	0.0012	17.3
0.0050	0.0007	20.8

NEON

DJ/DE*	Error	Energy+
0.0099	0.0022	13.8
0.0037	0.0010	15.3
0.0034	0.0008	17.5
0.00078	0.0003	21.4
0.00019	0.00007	31.3

MAGNESIUM

DJ/DE*	Error	Energy+
0.0097	0.0020	15.09
0.0064	0.0012	16.74
0.0027	0.0006	19.19
0.0015	0.0003	23.55
0.00026	0.00007	34.5

SILICON

DJ/DE*	Error	Energy+
C.0012	0.0004	17.7
0.00077	0.0002	24.1

SULPHUR

DJ/DE*	Error	Energy+
0.00048	0.0002	18.8
0.00005	0.00003	30.9

ARGON

DJ/DE*	Error	Energy+
0.0007	0.0005	16.8

*DJ/DE in units of particles/cm^2-sec-sterad-MeV/nucleon
+Energy in MeV/nucleon

data points with energy between 15 and 25 MeV/nucleon. Oxygen is used as a base for the abundance ratios as it is the species with the best flux determination. This power law fit yeilds a spectral index of 4.1.

Having an assumed spectral shape in the energy interval, it becomes a simple matter to scale the intensity of the oxygen spectrum to each flux datum point of each nucleus in the energy interval. The average value of these scaling factors weighted according to the statistics of each flux datum point, will then be the best estimate of if the abundance of that species relative to oxygen. These results are summarized in Table 2. The limits on the ratios expressed in Table 2 were calculated by assuming the entire uncertainty is statistical in nature. Each abundance ratio will be viewed as being appropriate at the mean energy of 18.4 MeV/nucleon in later discussions of energy variations of relative abundances. This value is the average energy for a power law spectrum with a spectral index of 4 for the mutual energy interval of 15 to 25 MeV/nucleon.

Also shown in Table 2 are the solar spectroscopic abundances compiled by Withbroe (1971) and the solar system abundances reported by Cameron (1973). The abundances reported by Cameron rely heavily on the elemental abundances obtained by the analysis of meteorites, particularly type I carbonaceous chrondrites (see also Mason, 1971). Cameron's abundances for carbon, nitrogen, and oxygen are also taken in part from the compilation by Withbroe (1971). The values Cameron reports for helium and neon, however, are taken from solar cosmic ray measurements reported by Bertsch et al. (1972).

TABLE 2 Abundances Relative to Oxygen

Element	This Experiment $15 \leq E/N \leq 25$	# of Particles $15 \leq E/N \leq 25$	Solar-Spectroscopic*	Solar System**	Solar System ÷ This Experiment
Helium	60±12	27	-	102	.59
Carbon	0.45 ±0.04	168	0.55	0.55	.82
Nitrogen	-	-	0.17	0.17	-
Oxygen	≡ 1.0	348	1.0	1.0	1.0
Neon	0.13 ±0.02	43	0.042	0.16	.81
Magnesium	0.25 ±0.03	87	0.052	0.049	5.1
Silicon	0.11 ±0.02	27	0.052	0.047	2.34
Sulphur	0.033±0.013	5	0.024	0.023	1.43
Argon	0.031±0.021	2	0.0066	0.0055	-
Calcium	<0.006+	0	0.0031	0.0034	-
Iron	0.06 ±0.015	22	0.040	0.043	1.4

* Withbroe (1971)
** Cameron (1973)
\+ 95% confidence

It is interesting to note that, with the exception of magnesium, the abundances measured in this experiment generally agree with the solar system abundances, if the large uncertainties are taken into consideration. In particular, the spectroscopic data are assigned uncertainties by Withbroe (1971) of about a factor of 2 with the exception of iron which has an uncertainty estimated to be about a factor of 3.

4. Discussion

A. The Energy Dependence of the Abundance Ratios

In order to study the dependence of the abundance ratios on energy, the results of this experiment are combined with many other solar particle composition measurements as shown in Figures 5 and 6. Where the experimental results were quoted with respect to medium nuclei rather than oxygen nuclei, a factor of 1.75 based on the ratio (C,N,O)/O summarized by Bertsch et al. (1972) is used to convert the abundance ratios to a similar reference species. The abundance measurements of heavy nuclei are reported in this summary for all known experiments where ratios were quoted between species observed in a common energy interval and hence insensitive to spectral extrapolation. For this reason, the results of Mogro-Campero and Simpson (1972) which are an average over 7 flares, are not plotted. Although all of the shown experiments measure fluxes over finite energy intervals, the following procedure has been adopted for plotting the data. If the measurements do not support a variation in abundance with energy, the abundances are plotted with a single point at the average energy of the measurements. The steep particle flux spectra cause the average energy of each observation to be close to the lowest energy measured.

The high energy measurements shown in Figures 5 and 6 have been made by the Goddard group with sounding rockets (e.g. see Bertsch et al., 1972, 1973a, 1973b, 1974; Biswas et al., 1962, 1965) or balloon (Biswas et al., 1966) exposures of nuclear emulsion.

Two separate results from the University of California, Berkeley group are shown in the figure. Crawford et al. (1972) report measurements in the January 25, 1971 flare which result from analysis of plastic detectors as mentioned earlier. The results reported by Braddy et al. (1973) are obtained from glass and plastic detectors exposed on the Apollo 16 spacecraft and reflect measurements during the solar flare in April 1972. The extensive observations of solar particles by this group have been summarized by Price et al. (1973).

The charge composition of solar particles emitted during the major solar flares in April and September 1971 was measured with a solid state telescope by Teegarden et al. (1973). This experiment had excellent charge separation and was able to measure nuclei from carbon through iron in a common energy interval between 13.5 and 47 MeV/nucleon. The results reported from this IMP-VI experiment are shown in the figures for each of the two flares for those nuclei where the results differ between the flares. Where the results from the two flares are in agreement, only the September measurement is shown because the larger particle fluxes in this flare yeilded smaller statistical uncertainties.

The data reported by Armstrong and Krimigis (1971) for 35 events during 1967 and 1968 are shown as the shaded area in Figure 5. These measurements were made with a single element dE/dX detector in the energy interval from 0.5 to 2.5 MeV/nucleon on the Explorer 35 satellite and show substantial variability in the helium-to-medium ratio between different solar particle events.

Energetic solar particles were also measured during a solar flare period from about October 29 and November 4, 1972 by Hovestadt et al.

(1973) in the energy interval between 0.62 and 6.9 MeV/nucleon. Energy spectra were obtained for carbon, oxygen, and iron nuclei. Interestingly, no energy dependence for the iron-to-oxygen ratio was observed within the uncertainties. The linear energy scale in the figures compresses the energy region of these measurements so only a single point is shown although the experiment was able to measure carbon, oxygen, and iron at several different energies. Gloeckler et al. (1973) have measured the enhancements of exygen, silicon and iron relative to helium at 100 keV/nucleon and find that these nuclei are overabundant by factors of 35 to 100.

These combined data allow the following observation to be made. The abundance measurements made during short sample periods with sounding rocket exposures are not systematically different from satellite measurements at the same energies. Thus if the abundances are time varying, this variation integrated over the entire flare yields the same essential result as a short exposure near the flare particle flux maximum. The enhancements of heavy nuclei relative to oxygen are also seen to be increasing with charge and decreasing with energy. However, while both the magnitude of the enhancements and the energy at which the enhancement occurs is variable from event to event, there is no apparent correlation with event size, solar location, or other event characteristic.

Further, the abundance variations seem to be decreasing with energy with the variation above 10 MeV/nucleon limited to within a factor of three. Although the high energy data are limited (there is only a single flux datum point above 100 MeV/nucleon), the observations are consistent with the concept that the highest energy particles are a representative sample of the solar atmosphere.

B. Solar Particle Acceleration and Propagation

The abundance ratios are calculated by comparing fluxes of nuclear species at the same energy/nucleon. If the nuclei are fully stripped, then the charge-to-mass ratios of all the nuclei compared in this work, with the exception of iron, have the same charge-to-mass ratio of 0.5. (Fully stripped iron has a charge-to-mass ratio of 0.46.) It follows that if these nuclei are compared at the same energy/nucleon, and are fully stripped, then the result is equivalent to a comparison at the same rigidities. This point is important since it enables the solar particle analysis to be considered from the separate viewpoints of propagation and acceleration.

The experimental evidence (Gleockler et al., 1973) suggests that at all the energies considered in this discussion ($\geq$ 10 MeV/nucleon), solar flare particles are fully stripped during the propagation process. As discussed in the introduction, particles with the same charge-to-mass ratio will be treated identically by macroscopic electromagnetic interactions. Adiabatic deceleration, however, will cause the energy/nucleon measured at the detector to be representative of a higher energy/nucleon at the start of the propagation process. Therefore, unless the abundance ratios are energy dependent as a result of the deceleration processes, the adiabatic deceleration will have no effect on the abundance ratios. The likely acceleration mechanism are variations on the Fermi (see Fermi, 1949, 1954, and Parker, 1955,

1957) or the betatron (see Swann, 1933 and Alfven, 1959) mechanism.

In attempting to relate the observations to the acceleration process, the simplest possibility would be that the abundance enhancements (at the energies measured in this experiment for example) are correlated with the first ionization potentials of the nuclei. This is suggested since the atoms in the solar atmosphere would be essentially unaffected by electromagnetic acceleration processes until at least the first electron was removed. Note, however, that this effect is very difficult to isolate from a general charge dependence because those elements for which spectroscopic measurements are available all have low ionization potentials which are similar in value. Helium and neon have singificantly larger ionization potentials and would provide a sensitive test of the correlation between ionization potential and enhancement of particle flux, but unfortunately spectroscopic data for these elements are lacking for the chromosphere and photosphere.

If the coronal value for neon (Withbroe, 1971) is compared with the results from this experiment, neon is seen to be overabundant in solar cosmic rays by a factor of 3, which is the opposite from the expected result as neon has a relatively high first ionization potential. Further, the only element more overabundant in this comparison than neon is magnesium, which has a low first ionization potential of 7.6 eV, therefore implying a lack of positive correlation with the first ionization potential. It should be noted that the solar system abundances of Cameron (1973) include values for helium and neon, but these values are taken from solar cosmic ray measurements at high energies and hence cannot be used for this analysis. In fact, as suggested by Hirshberg (1973), there is little reason to believe that the enhancements should be simply related to the first ionization potentials because, for a given stripping energy, the multicharged nuclei would be in varying degrees of ionization rather than being singly ionized. The resulting enhancements would then depend on the manner in which the particle accelerations depended on rigidity.

Consider now the effect of introducing a rigidity dependence into an acceleration mechanism acting on a confined solar region. If the particles which are accelerated have different rigidities at the same velocities (i.e. the nuclei are less than fully stripped), the acceleration mechanisms allow preferential leakage of partially stripped nuclei from the accelerating region when the gyroradii of the high rigidity particles become too large for containment. These particles would then yield abundance enhancements at low energies which increase with charge. Due to the very steep spectra, however, these particles would represent the bulk of the particles accelerated. The remaining particles subsequently accelerated to high energies would then be drawn from a sample of the solar atmosphere severely depleted as a function of increasing charge. The observations, however, imply that the high energy particles are a representative sample of the solar atmosphere.

One acceleration process consistent qualitatively with the observations would involve a balance between energy loss due to coulomb interaction and energy gain from the acceleration mechanism. While a particle undergoing, for example, a Fermi acceleration, will gain energy monotonically as a function of particle momentum, the energy loss rate will reach a maximum value at a low velocity, and then decrease due to the following effects. As the energy loss rate depends on the particle's charge, for very low particle velocities the small effective charge of the nucleus will cause the energy losses to be small. As the particle velocity increases, the equilibrium charge will increase causing the energy loss rate to increase. Once the atom is fully stripped, further increases in particle velocity will cause the energy loss rate to decrease approximately as inverse velocity squared.

The total energy gained by the particle will be the difference between the energy given to the particle by the acceleration mechanism and the energy lost as a result of the Coulomb collisions. At low energies these competing effects could lead to Z-dependent acceleration. At high energies, the acceleration process would dominate and effects due to energy loss would be negligible. It would seem, however, that an accelerating process which depends on the detailed balancing of these two effects would lead to greater flare-to-flare variation than is observed.

Another possibility is that the sample of particles being accelerated contains a component enriched with heavy nuclei. As a simple example, consider the accelerated material to consist of two particle populations. One is a representative sample of solar material located in the lower chromosphere where mixing is reasonably complete. The second, biased sample is residing in the upper chromosphere or corona where heavy elements may be enriched. If the solar acceleration process acts on both of these populations, but accelerates the lower population more strongly, perhaps because the fields are stronger in this lower region, particle distributions in agreement with the experimental evidence could be attained. It has been noted for example by Brandt and Hodge (1964) that heavier elements are expected to diffuse high into the chromosphere and lower corona and therefore become enhanced in these regions.

5. Summary and Conclusions

The detailed charge composition of heavy nuclei emitted during the January 25, 1971 solar flare were presented. The relative abundances were calculated for the energy interval from 15 to 25 MeV/nucleon without spectral extrapolations. When these data were combined with the results from other experiments a general picture of solar particle abundances as a function of energy emerged.

It has been noted that measurements made with short time exposures with sounding rockets yielded results essentially the same as satellite experiments which integrate over long time intervals when the comparisons are made at the same energies. Furthermore, although the abundances exhibit considerable variability at low energy, the variability at energies above 10 MeV/nucleon are limited to within a factor of three for variations from flare to flare and as a function of energy. In fact, the highest energy measurements are seen to be consistent with the measurements of the solar abundances obtained with spectroscopic techniques.

These observations, together with the established enhancements at low energies, place rather stringent constraints on the possible solar acceleration mechanism. The difficulty in correlating the solar cosmic ray abundances to the first ionization potentials has also been noted. Further, it does not appear that the inclusion of rigidity effects alone is sufficient to produce abundance ratios consistent with the observation. One possibility is that the solar acceleration process acts on regions of the solar atmosphere which are enriched with high charge elements relative to the "normal" solar composition nearer to the photosphere.

Acknowledgements

I would especially like to thank Dr. D. Bertsch (principal investigator for the SPICE experiment) and Dr. D. Reames for their illuminating suggestions and guidance. I, also, sincerely thank Dr. H. Crannell and Dr. C. Fichtel for their aid and guidance throughout the course of my thesis on which the contents of this paper are based.

REFERENCES

Alfven, H., 1959, Tellus 11, 106.

Armstrong, T. P. and Krimigis, S. M., 1971, J. Geophys. Res. 76, 4230.

Armstrong, T. P., Krimigis, S. M., Reames, D. V., and Fichtel, C. E., 1972, J. Geophys. Res. 77, 3607.

Bertsch, D. L., Biswas, S., and Reames, D. V., 1974, NASA X-662-74-32, submitted to Solar Physics.

Bertsch, D. L., Fichtel, C. E., Pellerin, C. J., and Reames, D. V., 1973a, Astrophys. J. 180, 583.

Bertsch, D. L., Biswas, S., Fichtel, C. E., Pellerin, C. J., and Reames, D. V., 1973b, Solar Phys. 31.

Bertsch, D. L., Fichtel, C. E., and Reames, D. V., 1972, Ap. J. 171, 169.

Biswas, S., Fichtel, C. E., and Guss, D. E., 1962, Phys. Rev. 128, 2756.

Biswas, S., Fichtel, C. E., Guss, D. E., and Waddington, C. J., 1963, J. Geophys. Res. 68, 3109.

Biswas, S., Fichtel, C. E., 1965, Space Science Reviews IV, 709, 736.

Biswas, S., Fichtel, C. E., and Guss, D. E., 1966, J. Geophys. Res. 71, 4071.

Braddy, D., Chan, J. and Price, P. B., 1973, Phys. Rev. Letters 30, 669.

Brandt, J. C. and Hodge, P. W., 1964, Solar System Astrophysics, McGraw Hill, New York.

Cameron, A. G. W., 1973, Space Science Reviews 15, 121.

Crawford, H. J., Price, P. B., and Sullivan, J. D., 1972, Astrophys. J. 175, L149.

Fermi, E., 1949, Phys. Rev. 75, 1169

Fermi, E. , 1954, Astrophys. J. 119, 1.

Fichtel, C. E., and Guss, D. E., 1961, Phys. Rev. Letters 6, 495.

Gloeckler, G., Fan, C. Y., and Hovestadt, D., 1973, 13th Int. Conf. Cosmic Rays, Univ. of Denver 2, 1492.

Heckman, H. H., Hubbard, E. L., and Simon, W. G., 1963, Phys. Rev. 129, 1240.

Hirshberg, J., 1973, Reviews of Geophysics and Space Physics 11, 115.

Hovestadt, D., Vollmer, O., Gloeckler, G., and Fan, C. Y., 1973, 13th Int. Conf. on Cosmic Rays, Denver 2, 1498.

Mason, B., 1971, Handbook of Elemental Abundances in Meteorites, Gordon & Breach Science Publichers, New York.

Mogro-Campero, A., and Simpson, J. A., 1972, Astrophys. J. 171, L5.

Parker, E. N., 1955, Phys. Rev. 99, 241.

Parker, E. N., 1957, Phys. Rev. 109, 1328.

Pellerin, C. J., 1974, Ph. D. Thesis, Catholic Univ. of America.

Price, P. B., Chan, J. H., Crawford, H. J., and Sullivan, J. D., 1973, 13th Int. Conf. Cosmic Rays, Univ. of Denver 2, 1479.

Swann, W. F. G., 1933, Phys. Rev. 43, 217.

Teegarden, B. J., von Rosenvinge, T. R., and McDonald, F. B., 1973 Astrophys. J. 180, 571.

Withbroe, G. L., 1971, The Menzel Symposium on Solar Physics, Atomic Spectra, and Gaseous Nebulae, ed. K. B. Gebbie (NBS Spec. Pub. 353), p. 127.

FIGURE CAPTIONS

Figure 1. Differential fluxes vs. energy. The open circles represent oxygen nuclei, the open squares represent carbon nuclei, the crosses represent magnesium nuclei and the triangles represent neon nuclei. The fluxes were measured at 1520 UT on January 25, 1971. The straight lines are for reference only and correspond to a spectral index of 3.5.

Figure 2. The spectral index as a function of charge for a power law spectrum fitted to each of the species shown in Figure 1 plotted. Also shown is a helium datum point from Bertsch et al. (1973a).

Figure 3. The differential fluxes of the less abundant nuclei are shown for the same exposure as Figure 1. The open circles represent silicon nuclei, the open squares represent sulphur nuclei, the triangles downward pointing represent iron nuclei from Bertsch et al. (1973a), and the upward pointing triangle represents argon nuclei. The straight lines represent a spectral index of 3.5 for reference purposes only.

Figure 4. The data from Crawford et al. (1972) and this experiment are compared. The circles represent this experiment and the squares represent the results of Crawford et al. (1972). Oxygen is represented by open symbols and silicon is represented by filled symbols.

Figures 5 and 6. The results from many experiments are combined to study the energy dependence of the abundance ratios. The target symbol refers to the results from emulsion measurements from the present work for the January 25, 1971 solar flare. The horizontal slashes represent the results of Teegarden el al. (1973) with the presence of a nearby numeral indicating (1) the April 1971 flare and (2) the September 1971 flare. Small solid dots represent the measurements of Crawford et al. (1972) in the January 1971 solar flare. X's represent the results reported by Biswas et al. (1962) for the November 1960 solar flare. Open squares represent the results of Bertsch et al. (1972) for the April 1969 solar flare. The filled-in squares represent the measurements of Hovestadt et al. (1973) in the October 1972 solar flare. The results of Braddy et al. (1973) from the April 1972 solar flare are shown as asterisk symbols without error bars. The downward pointing triangles represent measurements from Bertsch et al. (1973a) for (1) the September 1966 solar flare, and (2) the September 1971 solar flare. The results of Bertsch et al. (1973b) for the August 1972 solar flare are shown by upward pointing triangles. Finally, the balloon measurement reported by Biswas et al. (1966) during the July 1961 solar flare is shown with the semi-circle symbol.

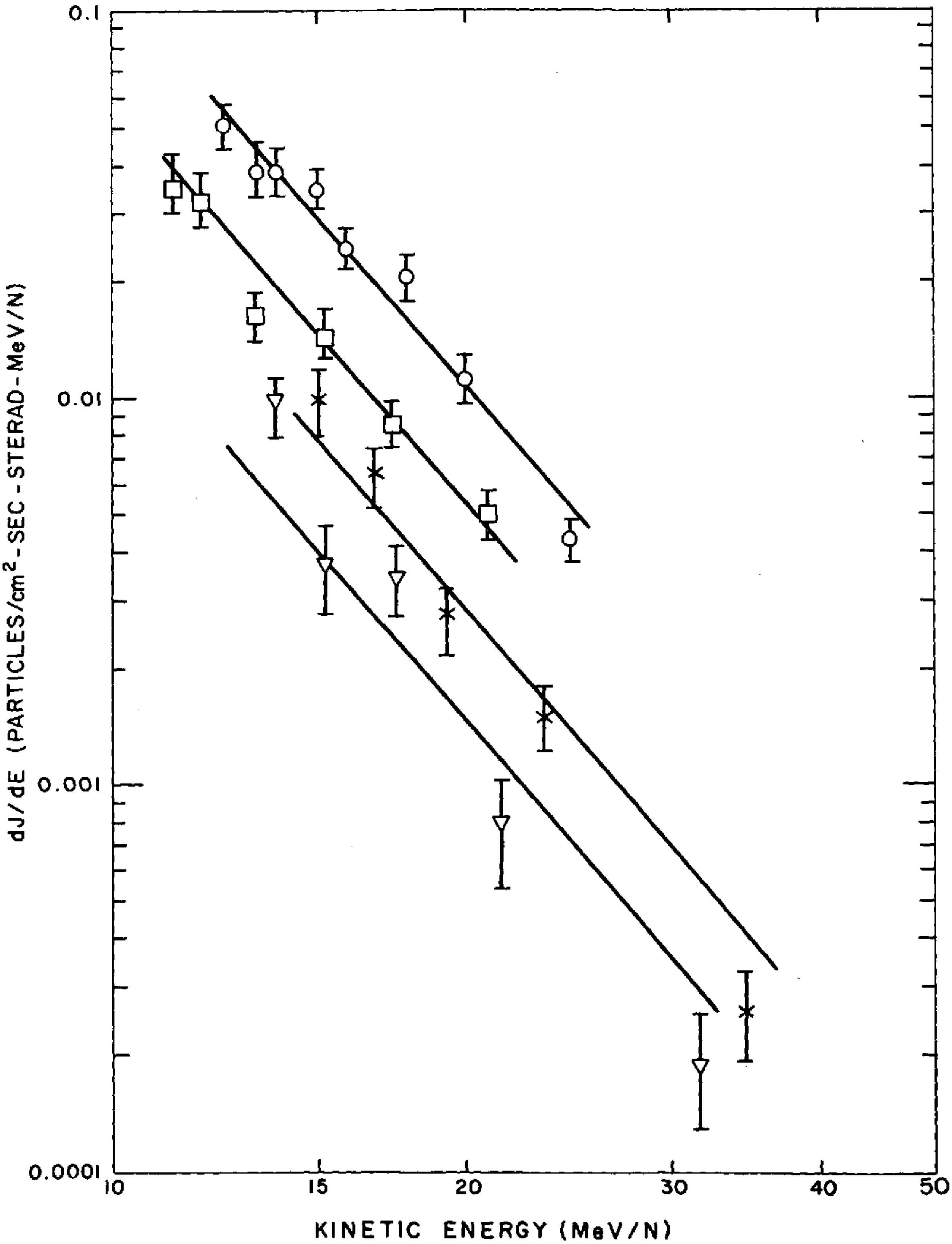
0.1
0.01
0.001
0.0001
dJ/dE (PARTICLES/cm2-SEC-STERAD-MeV/N)
10
15
20
30
40
50
KINETIC ENERGY (MeV/N)

Fig. 1

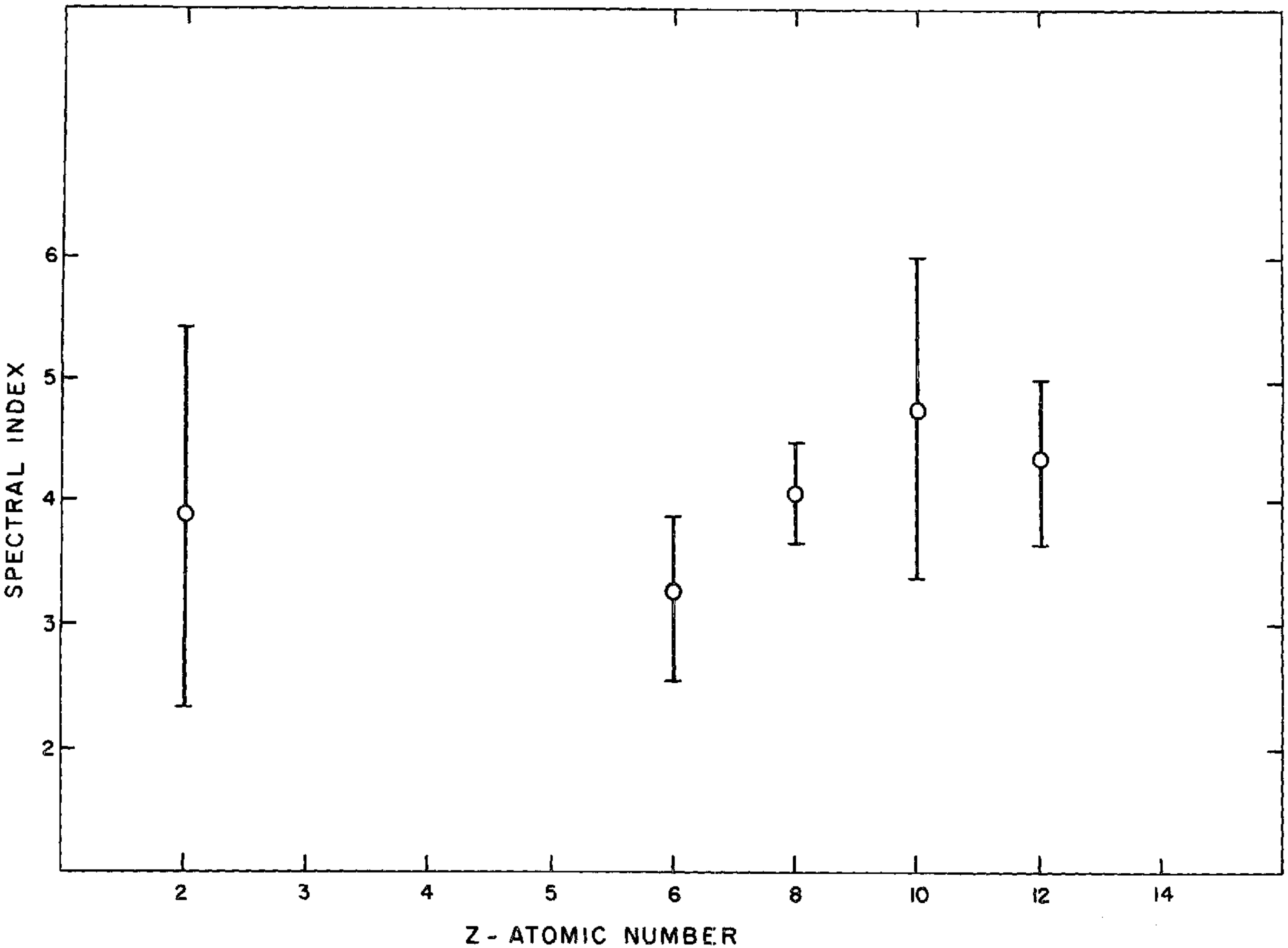

Fig. 2

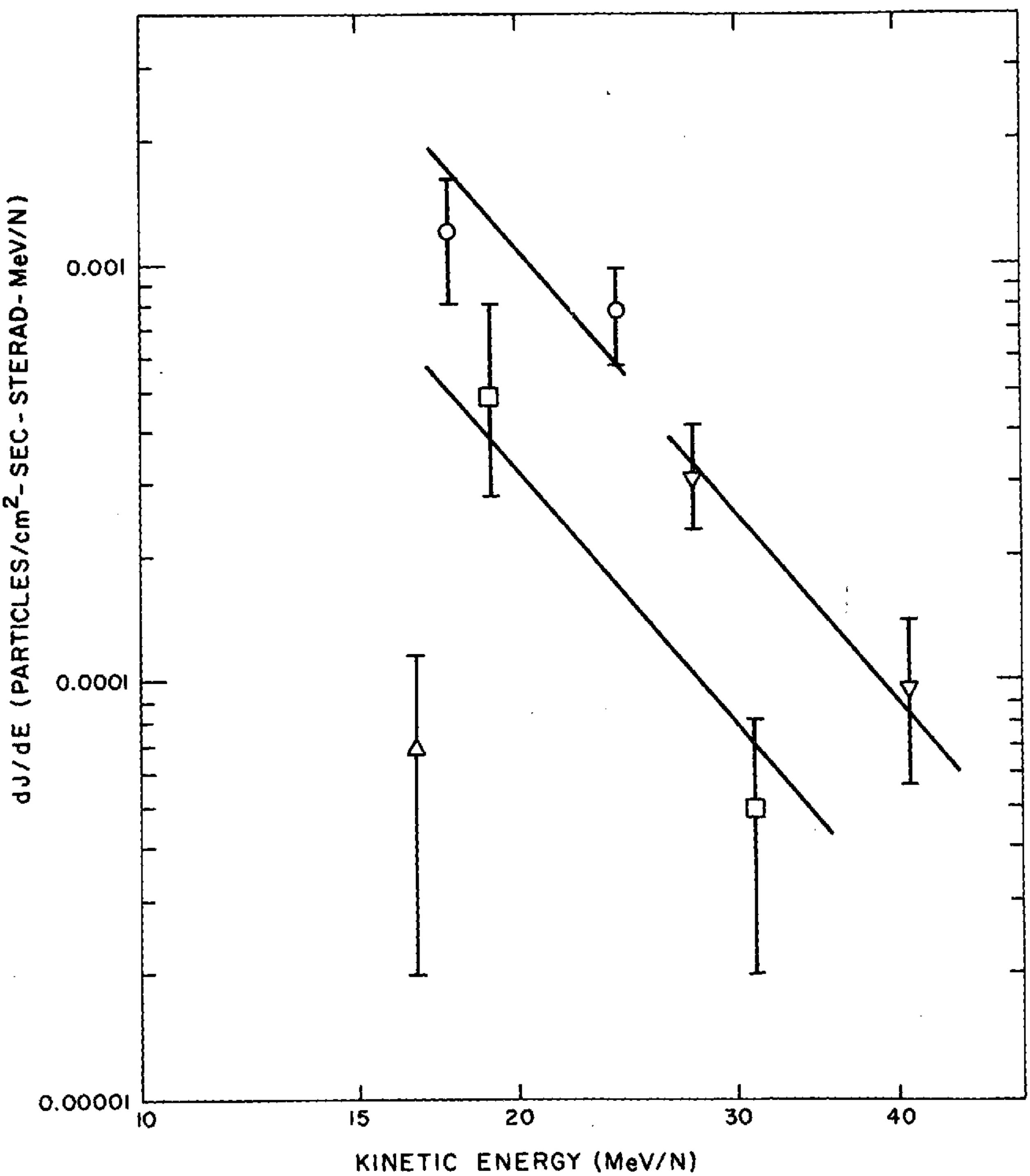
dJ/dE (PARTICLES/cm^2-SEC-STERAD-MeV/N)
0.001
0.0001
0.00001
10
15
20
30
40
KINETIC ENERGY (MeV/N)

Fig. 3

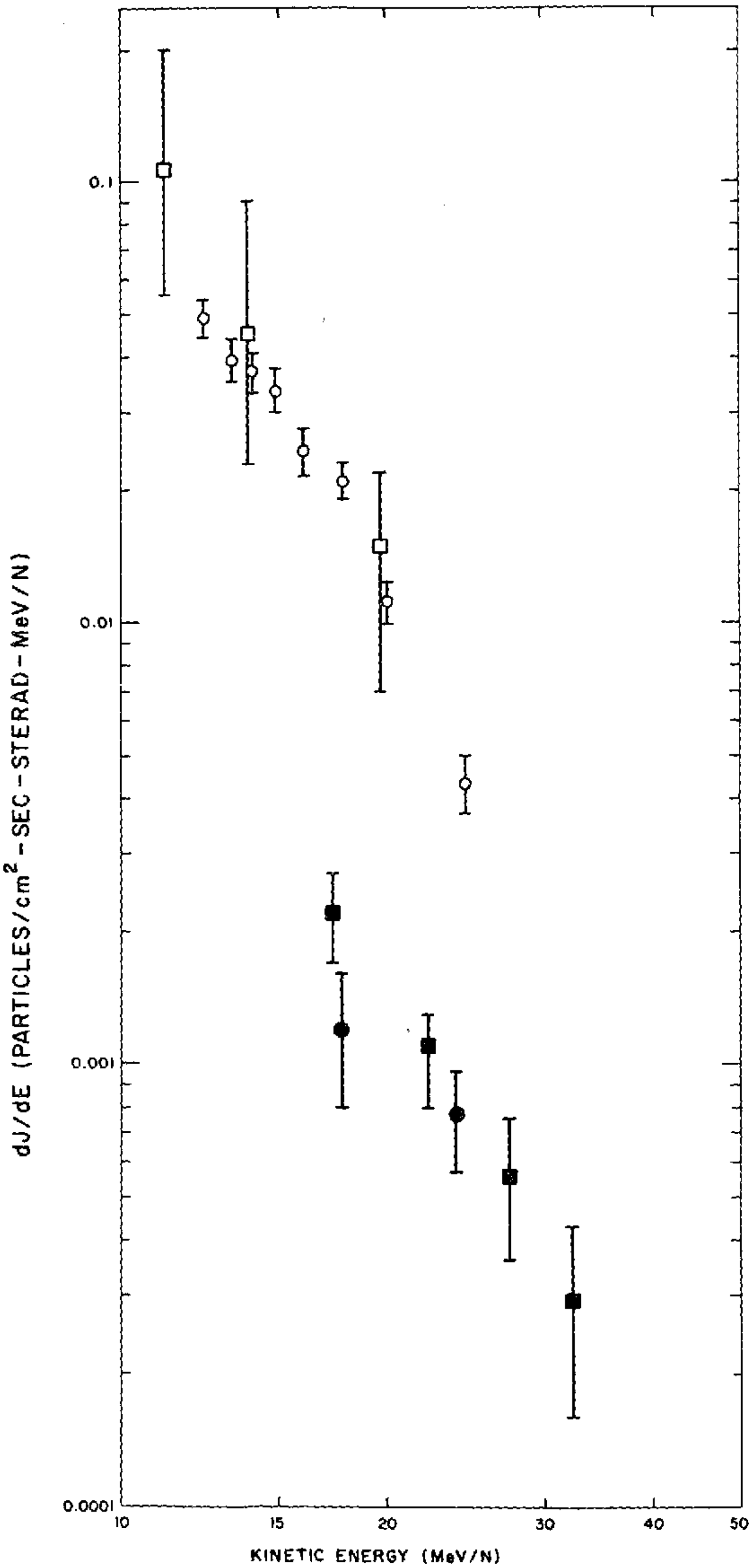
dJ/dE (PARTICLES/cm² - SEC - STERAD - MeV/N)
0.1
0.01
0.001
0.0001
10
15
20
30
40
50
KINETIC ENERGY (MeV/N)

Fig. 4

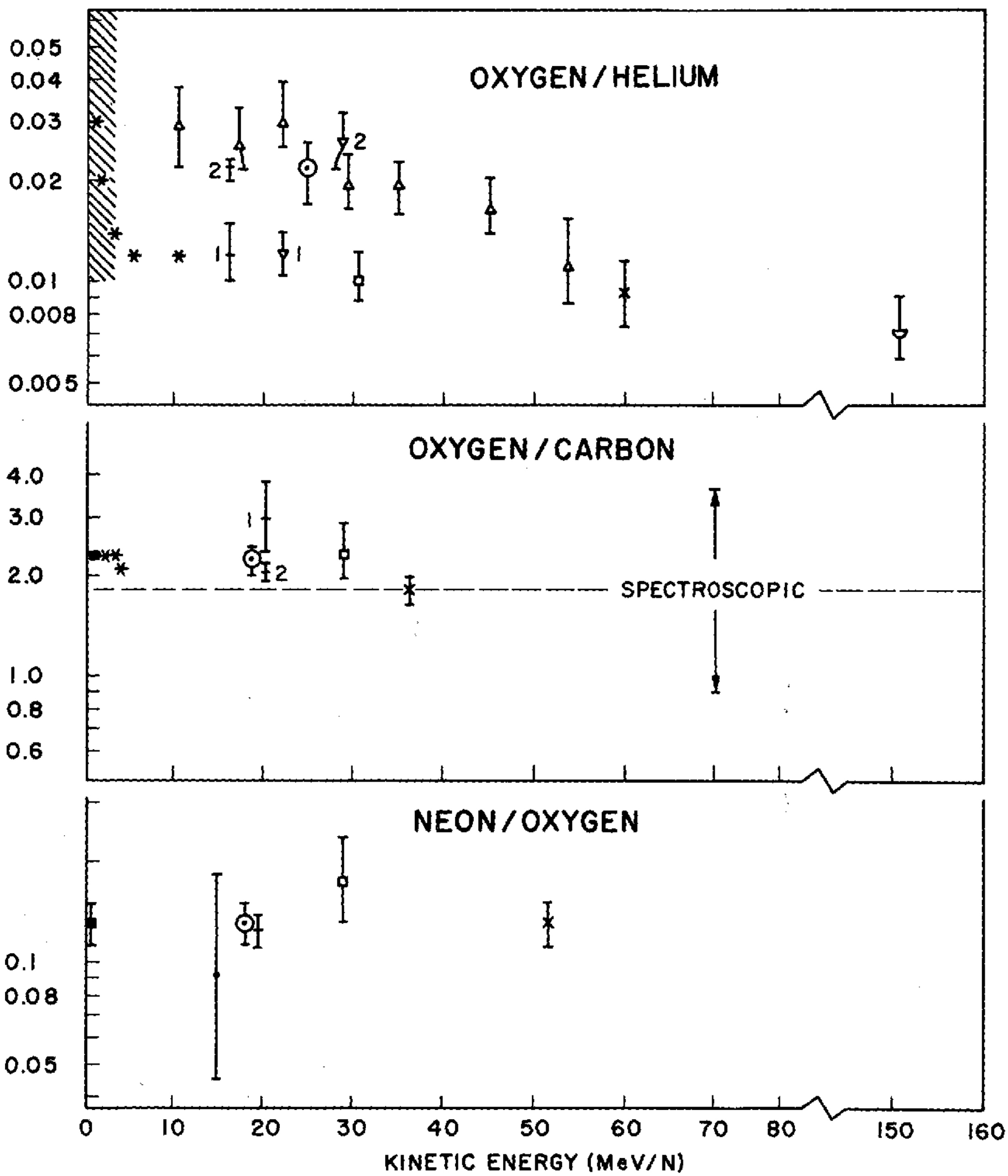
OXYGEN / HELIUM
0.05
0.04
0.03
0.02
0.01
0.008
0.005
OXYGEN / CARBON
4.0
3.0
2.0
1.0
0.8
0.6
SPECTROSCOPIC
NEON / OXYGEN
0.1
0.08
0.05
0
10
20
30
40
50
60
70
80
150
160
KINETIC ENERGY (MeV/N)

Fig. 5

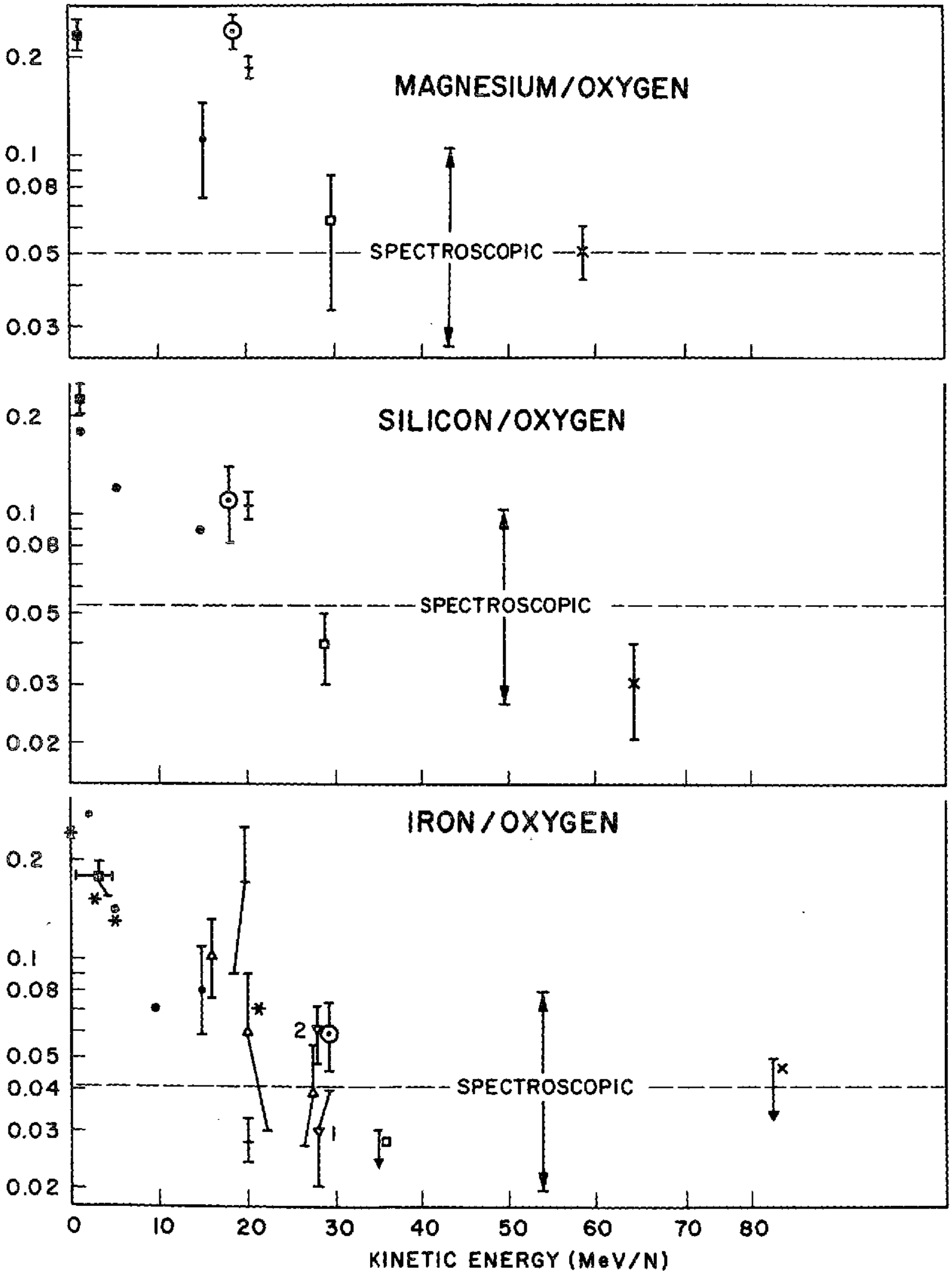

Fig. 6

NASA-GSFC